

Bioconjugated Fluorescent Polymeric Nanoparticles for Imaging and Targeted Therapy of HER2-Overexpressing Cancer Cells

Tzong-Der Way · Chi-Jung Chang · Cheng-Wen Lin

Received: 10 October 2010 / Accepted: 13 February 2011 / Published online: 1 March 2011
© Springer Science+Business Media, LLC 2011

Abstract We report the development of Herceptin-conjugated fluorescent polymeric nanoparticles (PNp) probes. Synthesis of fluorescent conjugated polymer as the core, preparation of the core/shell PNp, the ability of immobilizing Herceptin on PNp, targeting and imaging of bioconjugated PNp toward HER2-overexpressing cancer cells, and therapeutic effect on cell cycle, together with the expression of apoptosis related proteins, were investigated. We have achieved active tumor targeting by rapid PNp-antibody binding to tumor-specific antigens. Besides, Herceptin-conjugated PNp can suppress the growth of HER2-overexpressing cancer cells.

Keywords Nanoparticles · Imaging · Targeted therapy · Cancer cell · Fluorescent polymers

Chi-Jung Chang and Tzong-Der Way contributed equally to this work.

C.-J. Chang (✉)
Department of Chemical Engineering, Feng Chia University,
100, Wenhwa Road, Seatwen,
Taichung 40724, Taiwan
e-mail: changcj@fcu.edu.tw

T.-D. Way
Department of Biological Science and Technology, College of
Life Sciences, China Medical University,
91, Hsueh-Shih Road,
Taichung 40402, Taiwan

C.-W. Lin
Department of Medical Laboratory Science and Biotechnology,
China Medical University,
91, Hsueh-Shih Road,
Taichung 40402, Taiwan

Introduction

The development of noninvasive measures to identify cancer signatures, monitor drug delivery, and evaluate drug-induced effects in tumors has been a goal for enhancing cancer treatment [1]. As mechanisms related to tumor development are identified, signatures of these pathways are also very important in selecting effective therapeutics. The biofunctionalization of nanoparticles with the specific cell-targeting ligand offers the potential for delivery of therapeutic-loaded particles to a particular site or specific cell type in the body [2, 3]. Fluorescent nanoparticles can be used as sensitive and highly-specific probes for high-throughput screening, cellular biology and cell imaging. Various fluorescent nanoparticles, including colloidal inorganic semiconductor quantum dots (QDs) [4, 5] and dye-loaded latex particles [6] have been studied. QDs have been covalently linked to biorecognition molecules, such as peptides, antibodies, or nucleic acids, and image ligand-receptor to target the receptors [7].

However, there are potential concerns and limitations of using bioconjugated QDs probes. Because QDs are complexes of heavy metals, cytotoxicity is a critical problem in any live-cell or animal experiments [8]. For example, cadmium is both hepatotoxic and nephrotoxic. Heavy metals can poison normal enzymes by competing with cofactors. They cause cell death at sufficiently high levels. The cytotoxic effects of QDs may be mediated by cadmium ions (Cd^{2+}) released from the QDs cores. CdTe QDs induce cell death accompanied by lysosomal enlargement and intracellular redistribution via mechanisms involving both Cd^{2+} and reactive oxygen species. Moreover, Chang et al. [9] studied the cytotoxicity of different surface-coated CdSe/CdS QDs

based on diverse levels of exposure with extracellular and intracellular nanoparticle in cells. The exposure concentration that leads to equivalent QDs uptake in cells for different surface-modified QDs showed no statistical difference in cytotoxicity with the bare. Dye-loaded nanoparticles have been shown to be limited in dye-loading concentration due to self-quenching. The dye leakage from the matrix in the dye-doped nanoparticles is also a problem. The π -conjugated polymer can be used for in-vivo observation of the degradation of postsurgical anti-adhesion films [10, 11]. The use of encapsulated π -conjugated polymer particles as fluorescent labels is a promising alternative. Many π -conjugated polymers are known to possess high fluorescence quantum yields and high extinction coefficients [12]. Wang [13] reported the lipid-modified conjugated polymer nanoparticles for cell imaging and transfection.

Herceptin, a humanized monoclonal antibody targeting the HER2 receptor, was approved by the FDA in 1998. Amplification of the *HER2* gene (alternatively known as *neu* or *ErbB2*) or overexpression of HER2 protein was found in up to 30% of breast carcinomas [14]. Patients whose breast tumor cells overexpress HER2 have poor clinical outcome, such as shorter survival or earlier relapse [15]. HER2 overexpression has been shown to enhance proliferative, pro-survival, and metastatic signals in breast cancer cell lines. HER2-mediated signaling has also been reported to result in resistance to apoptosis induced by many stimuli [16]. Additionally, repressing HER2 overexpression attenuates its antiapoptotic signaling and suppresses HER2-mediated malignant phenotype. HER2 is not only a potent oncogene but also an excellent therapeutic target in breast cancer. The importance of HER2 in breast cancer led to the development of agents that aimed at reducing HER2 level or activity [17].

In this study, fluorescent polydioctylfluorene-benzothiadiazole-bis(2-thiophenyl) benzothiadiazole copolymer (PFBTTB) PNp was synthesized and conjugated with Herceptin to make a PNp probe suitable for targeting and imaging of HER2-overexpressing cancer cells. This PNp probe contained the fluorescent polymer as a core. The surface of the PNp was modified by covalent attachment of Herceptin for tumor antigen recognition and multiple PEG segments for biocompatibility. The imaging, targeting, and therapeutic effect of bioconjugated PNp toward HER2-overexpressing cancer cells were studied.

Materials and Methods

Synthesis of PFBTTB Copolymer

The following monomers 2,7-dibromo-9,9-dioctyl-9 H-fluorene (0.5 g), 4,7-dibromobenzo [1, 2, 5] thiadiazole (0.08 g),

4,7-bis(5-bromothiophen-2-yl) benzo [1, 2, 5] thiadiazole (0.058 g), 4,4,5,5-tetramethyl-2-(2-(4,4,5,5-tetramethyl-1,3,2-dioxaborolan-2-yl)-9,9-dioctyl-9 H-fluorene -7-yl)-1,3,2-dioxaborolane (0.625 g), 2 mol% Pd(pph₃)₄ catalyst and toluene (40 mL) were added into a 150 mL flask. The mixture was stirred until all ingredients were dissolved. A sodium carbonate solution (2 M, 0.07 mL) was added and the solution was heated at 95 °C for 16 h prior to addition of 0.5 ml of bromobenzene. The polymer solution was precipitated with 500 mL methanol. The red PFBTTB polymer was dried under vacuum at 60 °C. The yield of the polymer is 30%. The molecular weight (M_n) is 18550 (polydispersity=2.7).

Synthesis of AEI Dispersant

1,2-epoxydodecane, (0.22 g) and polyethylenimine (0.60 g PEI, linear M_n=423, Aldrich, CA no. 29320-38-5) were mixed and then heated at 100 °C for 6 h to synthesize the amine-terminated AEI dispersant. IR (KBr): 912 (epoxy ring) disappear.

Synthesis of AEO Dispersant

After being vacuum-dried at 40 °C for 1 h, poly (ethylene glycol) methyl ether (0.45 g, M_n=350) and dodecyl isocyanate (0.27 g) were mixed in a flask and then heated at 80 °C under nitrogen atmosphere for 7 h. IR (KBr): 2260 (NCO) disappears, 1715 (urethane, NHCOO) forms.

Nanoparticle Preparation

A solution containing conjugated polymer PFBTTB (10^{-4} g), AEI (3×10^{-6} g), AEO (3×10^{-6} g), cetyl trimethylammonium bromide (CTAB, 3×10^{-6} g), and 10 ml THF was prepared. Such solution (10 mL) was added to deionized water (40 mL) under ultrasonic agitation. Then, THF was removed by partial evaporation under vacuum to make the nanoparticle dispersion.

Antibody Conjugation

The nanoparticle was conjugated with the Herceptin antibody (Chugai Pharmaceuticals Co.). Nanoparticle dispersion (125 μ L) was activated with heterobifunctional cross-linker of 4-(maleimidomethyl)-1-cyclohexanecarboxylic acid *N*-hydroxysuccinimide ester (SMCC) (14 μ L) for 1 h at room temperature. Herceptin antibody (300 μ L (1 mg/mL)) was reduced and fragmented by dithiothreitol (DTT) (6.1 μ L) for 30 min at room temperature. After the removal of excess SMCC and DTT by the desalting column, activated nanoparticles were covalently coupled with reduced antibody to react for 1 h. The conjugation reaction was then finished

with addition of β -mercaptoethanol (6.1 μ L, 7.5 μ M) for 30 min.

Characterization Methods

The size, shape, and morphology of the particles were characterized by Hitachi H-7500 Transmission Electron Microscope (TEM). The photoluminescence spectra and UV–vis absorption spectra were measured by the PL2006 Multifunction Fluorescent Spectrometer (Labguide co.).

Cell Culture

The NIH3T3 cells were grown in Dulbecco's Modified Eagle's Medium (DMEM) (Invitrogen) supplemented with 10% fetal bovine serum (FBS) (Invitrogen). The MCF-7 cells were cultured in DMEM containing 10% FBS. The MCF7/HER18 and 435.eB cells, which had been transfected to express HER2, were cultured in DMEM containing 10% FBS and 0.5 mg/mL G418 (geneticin) to select for HER2-expressing cells. The MDA-MB-435 cells were cultured in DMEM/F12 containing 10% FBS. All culture media were supplemented with penicillin/streptomycin (100 U/ml) and fungizone (2 mg/ml).

Cell Viability

Cells were treated with various doses of nanoparticles for 24 h before examining cell proliferation by MTT assay according to the manufacturer's instructions (Promega, Madison, WI). The absorbance was measured at 590 nm. The cell viability of the treated cells is expressed as the percentage of that of the control (defined as 100%). Data are shown as means \pm S.E. for three separate experiments.

Confocal Microscopy

After treatment, cells were fixed with methanol, blocked with 3% bovine serum albumin, stained with anti- β -tubulin monoclonal antibody, and then FITC-conjugated antimouse IgG antibody. Nuclear staining was done with 4,6-diamidino-2-phenylindole (DAPI). Cells were imaged with Leica TCS SP2 Spectral Confocal System.

Flow Cytometry

The cell cycle analysis was determined by flow cytometry. Cells were cultured in 60-mm Petri dishes and incubated for various times. After being trypsinized and washed twice with ice-cold PBS, the cells were fixed with 70% ice-cold ethanol overnight at -20 °C. After centrifugation, the cell pellets were treated with RNAase A and exposed to PI, and then analysed by flow cytometry (FACScan, BD Biosciences).

Western Blotting

Cells were treated with various agents as indicated in figure legends. After treatment, Western blotting was done as described previously [18]. Expression levels of PARP, cleaved caspase 3, and β -actin were detected by using specific antibodies in combination with enhanced chemiluminescence (ECL, Amersham, Arlington Heights, IL).

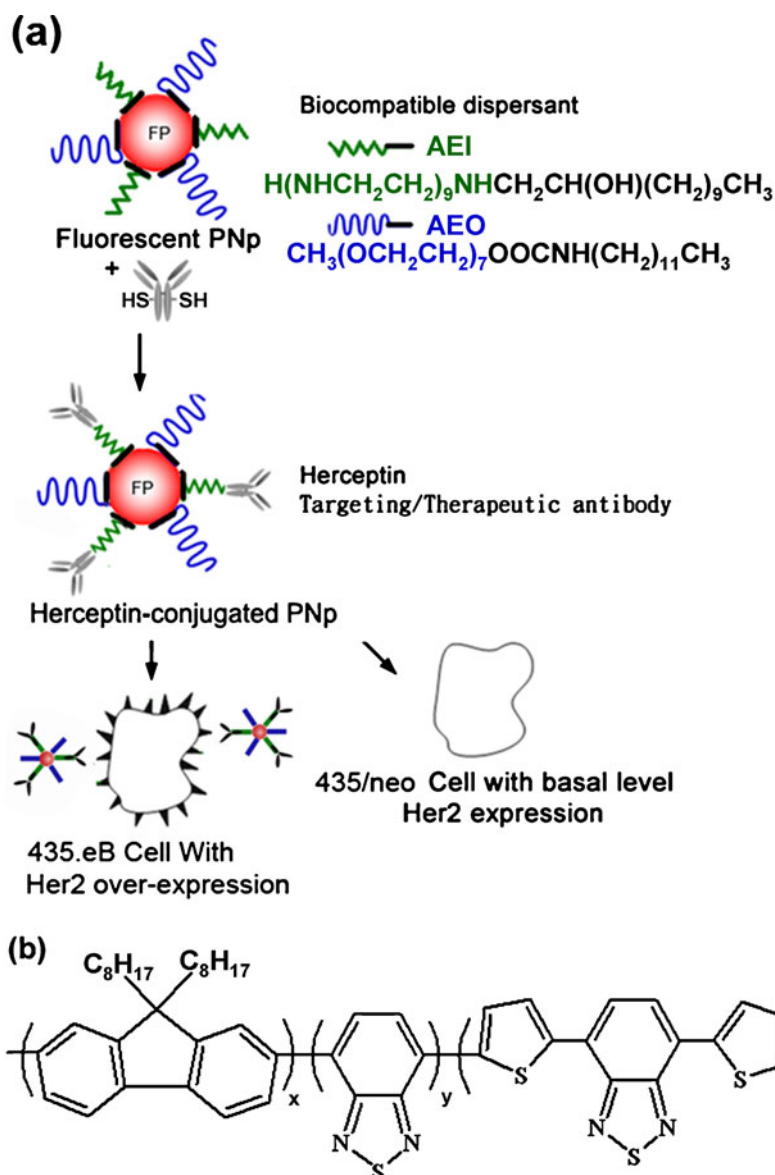
Results and Discussion

Figure 1a shows the structure of a multifunctional PNp probe that consists of the emulsifier AEI (with hydrophilic polyethylenimine and hydrophobic aliphatic carbon segments), emulsifier AEO (with hydrophilic polyethylene glycol and hydrophobic aliphatic carbon segments), and tumor-targeting ligands (Herceptin). The emulsifiers can disperse the fluorescent polymeric core. In addition, Herceptin can be conjugated on the amino groups of AEI dispersants. Whereas the hydrophobic aliphatic segment is attached to the fluorescent PFBTTB polymer core (Fig. 1b) through hydrophobic interactions between emulsifier and the polymer hydrocarbon, the hydrophilic segments (polyethylene glycol or polyethylenimine) extend toward the water medium.

Characteristics of Nanoparticles

Dispersions of conjugated polymer PFBTTB nanoparticles were prepared. The PNp aqueous dispersions were clear (not turbid), with colors similar to those of the polymers in THF solution. The aqueous PNp dispersion exhibits 88 nm red-shifted fluorescence (Fig. 2a, black line) and similar absorption spectra (Fig. 2b, black line) as compared to those of the polymer/THF solution (red line). The absorption spectrum of the PNp exhibits a change in the relative intensity of the peak and shoulder as compared to the spectrum of the polymer in solution. However, the peak maxima locate at nearly the same wavelength. These similar absorption peaks indicates that an overall decrease in the conjugation length [19] resulting from the bending or kinking of the polymer backbone did not occur. The fluorescence spectrum of PNp is red-shifted by 85 nm, as compared to those of the polymer in THF solutions. Since the nanoparticles possess a compact conformation, the molecular chain of fluorescent PFBTTB polymer is closely packed within the nanoparticle. The red-shift in fluorescence could be attributed to increased interactions between segments of the polymer chain, leading to energy transfer to low-energy chromophores and weakly fluorescent intrachain aggregates [20]. In vivo imaging using visible light is hindered by native biological fluorescence as well as light

Fig. 1 a Schematic illustration of Herceptin-conjugated polymeric fluorescent nanoparticle probes for in vitro cancer targeting and imaging and **b** chemical structure of fluorescent conjugated polymer (FP) PFBTTB



absorption by biological tissue constituents, such as amino acids and blood hemoglobin. However, red and near-IR-emitting fluorescence imaging can overcome these challenges because native biological fluorescence and absorbance are kept at their minima in the wavelength range of 600–900 nm [21]. Therefore, the above-mentioned red-shift of the PFBTTB nanoparticle probe makes it suitable for in vivo fluorescent imaging applications. The polymeric nanoparticles were well-dispersed by the dispersants. Their particle size distribution and optical properties (e.g., absorption spectra and emission spectra) did not change at least for 3 months. The size and morphology of nanoparticles were analyzed by TEM. Figure 3 shows the TEM image of Herceptin-conjugated PNp. The nanoparticles exhibit roughly spherical morphology. The diameters of the particles range from 70 nm to 120 nm. Since the

backbone of conjugated polymer is a rigid structure, the observation of approximately spherical morphology is interesting. Taking into account the large interfacial surface tension between the polymer and water, a roughly spherical polymer conformation is thermodynamically favored [22]. The fluorescent nanoparticles (PFNP) were made by acrylate polymer with embedded fluorescent dye and used for cancer imaging application [23]. The fluorescence emission maximum of PFNP shifted 6 nm to the longer wavelength compared with that of the dissolved dye.

Cytotoxicity of Nanoparticles

Since the PFBTTB PNp is to be used for biomedical applications, the issue of cytotoxicity has to be addressed. The viability of the fibroblast NIH3T3 cells in the presence

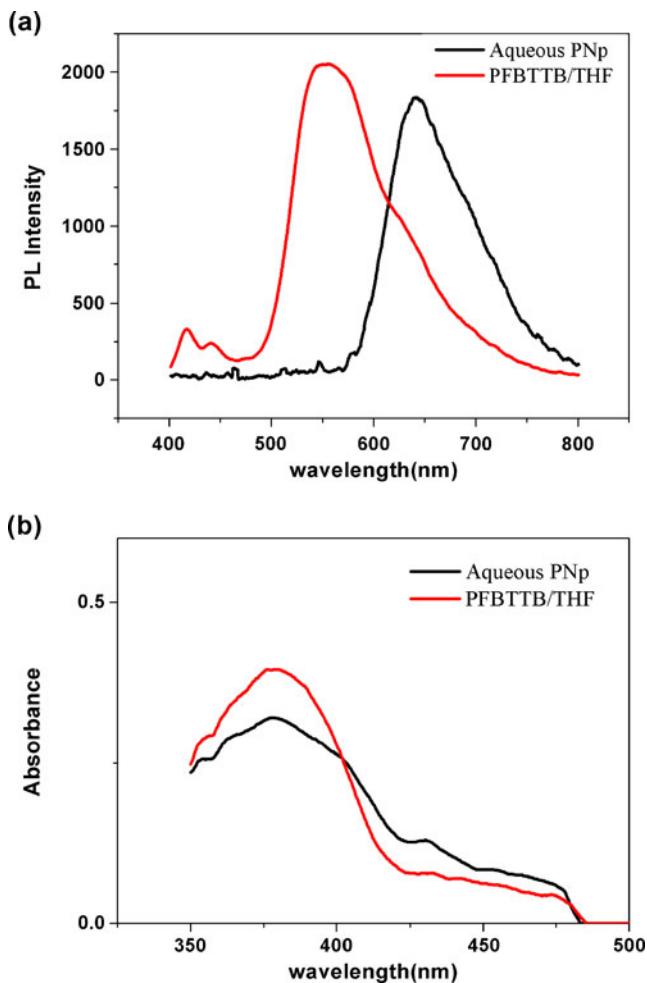


Fig. 2 a Photoluminescent b absorbance spectra of the aqueous PNp dispersion and PFBTTB polymer/tetrahydrofuran

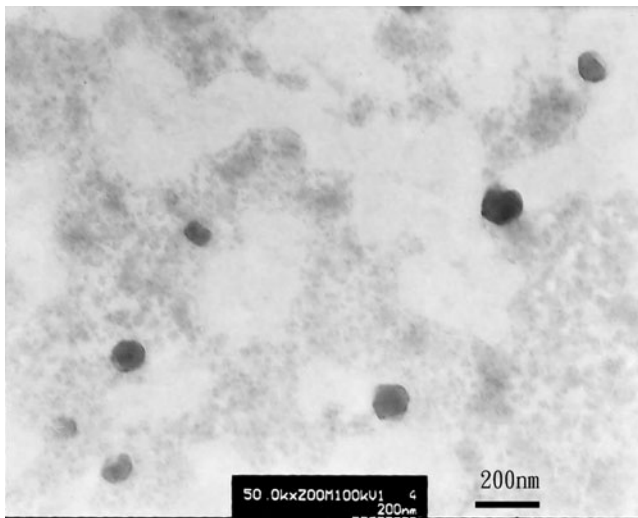


Fig. 3 TEM image of Herceptin-conjugated PNp

of PFBTTB PNp was assessed relative to cells in the control experiment (in the absence of PFBTTB) using the MTT assay, which has been described as a very suitable method for the detection of biomaterial toxicity. As shown in Fig. 4, the viability of cells remains high as compared to that of the nontoxic control after 24 h of incubation. This confirms the low toxicity of the PNp to fibroblast NIH3T3 cells.

Imaging and Targeting of Cancer Cells

The PNp consisting of red-fluorescent light emitting polymer (PFBTTB) encapsulated within the biocompatible polymer would facilitate tracking the delivery of the conjugated Herceptin. Moreover, binding of Herceptin mAb to its antigen promotes rapid internalization of the antibody, typically via receptor-mediated endocytosis, in principle, the immunocomplex along with the particle is also expected to trigger internalization and be subsequently directed into a vesicular compartment within the cell. Hence, the uptake of Herceptin-conjugated luminescent PNps in cells is able to be monitored effectively with the aid of laser confocal microscopy, which was adopted for analysis. It appeared that the PNp labeled with HER2 antibody was specifically targeted to the HER2 receptors on the surface of MCF7/HER2 (Fig. 5a) and 435.eB cells (Fig. 5b), which over-express HER2 receptors. As the incubation time increased, stronger emission was observed. On the other hand, no such binding of PNp to MCF7/neo (Fig. 5a) and 435/neo cells (Fig. 5b), which have lower expression of HER2 receptors, was observed. Moreover, PEG segments of AEO appeared to have no interference with antibody binding on AEI at its current level of conjugation, as confirmed by the targeting of PNp probe to cancer cells. This is in disagreement with the report that substantial interference with ligand binding could occur, which was thought to be attributed to the use of higher PEG densities or longer chains [24].

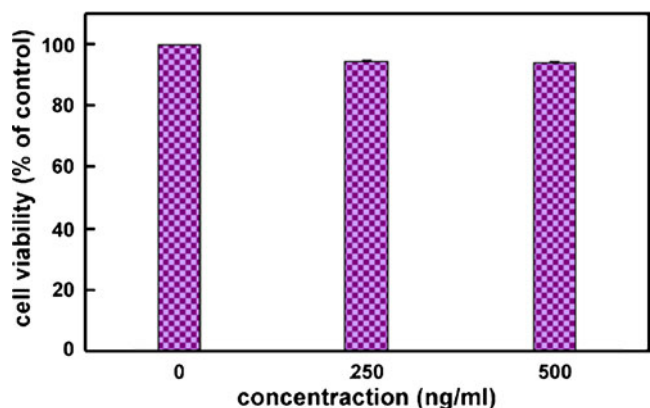
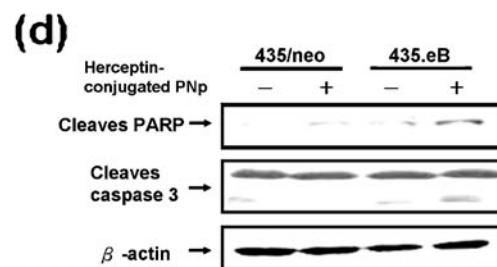
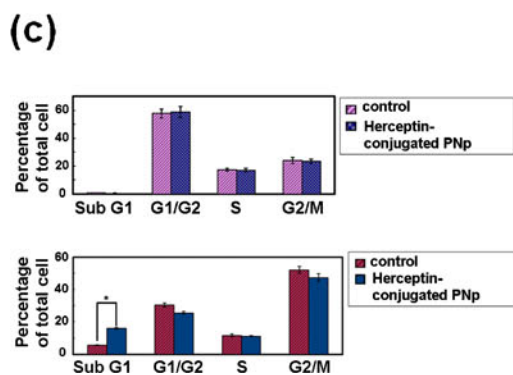
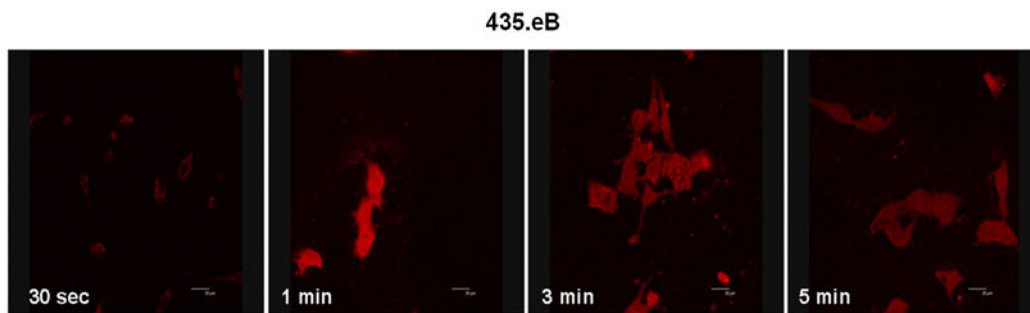
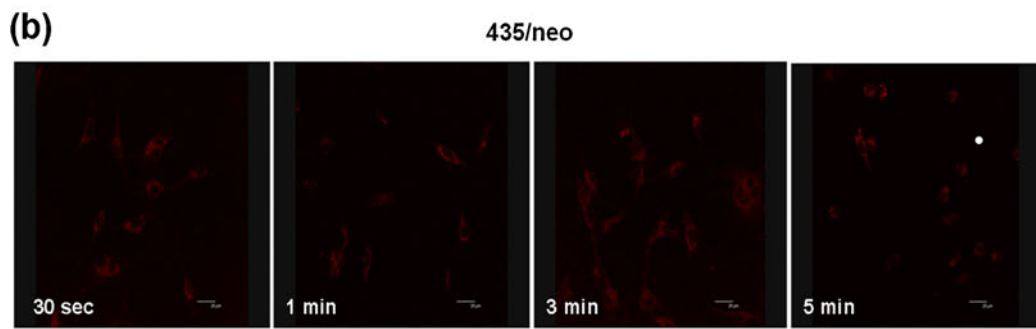
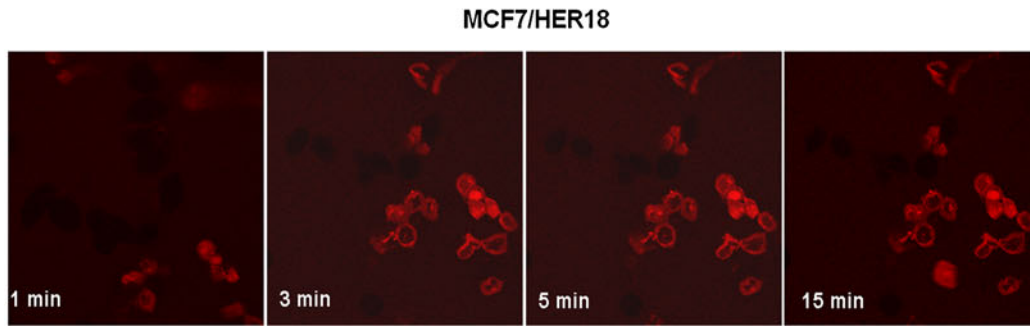
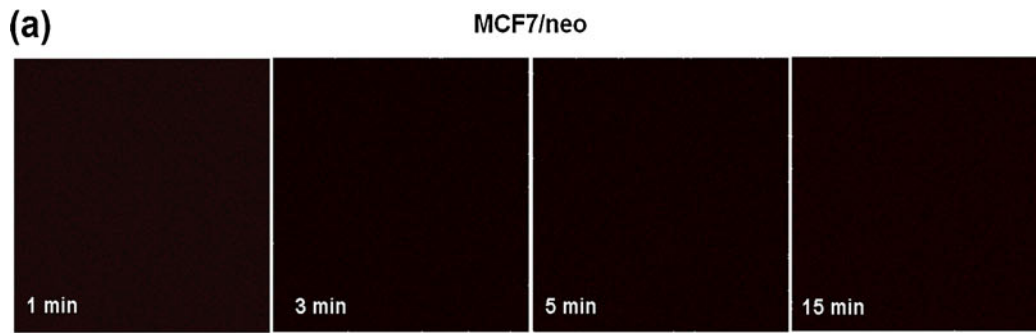


Fig. 4 Cytotoxicity of PFBTTB conjugated polymer on NIH3T3 cells



◀ **Fig. 5** The proliferation-inhibitory effect of Herceptin-conjugated PNp on HER2- overexpressing cells. **a, b** The specific targeting of Herceptin-conjugated PNp to HER2-overexpressed cells assessed by laser confocal microscope. **c** The cell cycle distribution of 435/neo and 435.eB cells treated with Herceptin-conjugated PNp for 24 h. **d** Detection of cleaved caspase-3 and PARP in the 435/neo and 435.eB cells treated with Herceptin-conjugated PNp for 24 h

Targeted Therapy of Cancer Cells

Herceptin is a recombinant humanized monoclonal antibody for the treatment of metastatic breast cancer by directly targeting against the extracellular domain of HER2. To determine the ability of Herceptin-conjugated PNp to change cell cycle progression or induce apoptosis on HER2-overexpressing cells, the propidium-iodide stain with flow cytometry was used to measure distribution of DNA contents among cells. The cell cycle in eukaryotes is classified into four phases: G1—gap phase and preparation of the chromosomes for replication; S—synthesis of DNA and centrosomes; G2—preparation for mitosis; and M—mitosis. Upon completion of one round of cell cycle, a cell is divided into two daughter cells. Each cell has a complete set of genes. Therefore, the inhibition in proliferation should be reflected in the cell cycle. Moreover, the increase in sub-G1 cells indicates cells undergoing apoptosis. Figure 5c illustrates the cell cycle distribution of 435/neo and 435.eB cells treated with Herceptin-conjugated PNp for 24 h. The indicated percentages are the mean of three independent experiments, each in duplicate. Flow cytometric analyses revealed a significant increase in the percentage of apoptotic sub-G1 fraction in Herceptin-conjugated PNp-treated cells as compared to the untreated control 435.eB cells. However, no significant change was observed in the 435/neo cells.

To verify the increase of sub-G1 fraction of 435.eB cells after treatment of Herceptin-conjugated PNp is indeed resulted from the induction of apoptotic pathway, we examined the expression of apoptosis related proteins by Western blot. The 435/neo and 435.eB cells were treated with Herceptin-conjugated PNp for 24 h. Cells were then harvested and lysed for detection of cleaved caspase-3 and PARP by Western blotting. The β -actin was used as an internal control. Data presented are representative of those obtained in at least three separate experiments. It has been known that the final pathway leading to execution of the death signal is the activation of a series of proteases termed caspases. The intrinsic and extrinsic apoptotic pathways converge to caspase-3, which cleaves the inhibitor of the caspase-activated deoxyribonuclease for the activation of the deoxyribonuclease that leads to nuclear apoptosis [25]. Moreover, poly ADP-ribose polymerase (PARP) is known to mediate post-translational modification of proteins playing crucial roles in many processes, including DNA repair

and cell death [26]. During apoptosis, whereas caspases cause PARP cleavage and inactivation, caspases themselves, including caspase-3, are part of cascade of cleavage and activation. Therefore, the cleavage of caspase-3 and PARP was used as an indication of cells undergoing apoptosis in our assay. After the treatment of Herceptin-conjugated PNp, an apparent cell apoptosis was observed in 435.eB cells, showing cleavage patterns of caspase-3 and PARP in the immunoblotting analysis (Fig. 5d). Overall, these results suggest that Herceptin-conjugated PNp preferentially suppresses the growth of HER2-overexpressing cancer cells.

Conclusion

We have developed a new kind of fluorescent, photostable PNp from the conjugated polymer, PFBTTB. The PNp can be modified by biorecognition molecules, Herceptin. The diameters of the nanoparticles range from 70 nm to 120 nm. The PFBTTB nanoparticle probe with a fluorescent emission at 645 nm is suitable for in vivo fluorescent imaging applications. Herceptin-conjugated fluorescent PNp were developed as probes suitable for targeted therapy and imaging of HER2-overexpressing cancer cells. The cellular toxicity test confirms the low toxicity of the PNp to fibroblast NIH3T3 cells. We have achieved active tumor targeting by rapid PNp-antibody binding to tumor-specific antigens. Herceptin-conjugated PNp are seen on the HER2 over-expressing cells (MCF/HER18 and 435/HER2 cells) but not on the HER2 basal cells (MCF7/neo and 435/neo cells). Meanwhile, Herceptin-conjugated PNp can suppress the growth of HER2-overexpressing cancer cells. These results open new possibilities for polymeric fluorescent nanoparticles as sensitive and low-cytotoxicity biomarkers in targeted therapy and imaging of cancer cell.

Acknowledgements The authors would like to thank the financial support from the National Science Council, Feng Chia University and China Medical University.

References

1. Nicolette CA, Miller GA (2003) The identification of clinically relevant markers and therapeutic targets. *Drug Discov Today* 8 (1):31–38
2. Sun C, Sze R, Zhang M (2006) Folic acid-PEG conjugated superparamagnetic nanoparticles for targeted cellular uptake and detection by MRI. *J Biomed Mater Res A* 78A(3):550–557
3. Toublan FJJ, Boppart S, Suslick KS (2006) Tumor targeting by surface-modified protein microspheres. *J Am Chem Soc* 128 (11):3472–3473
4. Yu X, Chen L, Deng Y, Li K, Wang Q, Li Y, Xiao S, Zhou L, Luo X, Liu J, Pang D (2007) Fluorescence analysis with quantum dot

- probes for hepatoma under one- and two-photon excitation. *J Fluoresc* 17(2):243–247
5. Xue FL, Chen JY, Guo J, Wang CC, Yang WL, Wang PN, Lu DR (2007) Enhancement of intracellular delivery of CdTe quantum dots (QDs) to living cells by tat conjugation. *J Fluoresc* 17(2):149–154
 6. Yang CS, Chang CH, Tsai PJ, Chen WY, Tseng FG, Lo LW (2004) Nanoparticle- based in vivo investigation on blood–brain barrier permeability following ischemia and reperfusion. *Anal Chem* 76(15):4465–4471
 7. Zhao Y, Liu S, Li Y, Jiang W, Chang Y, Pan S, Fang X, Wang YA, Wang J (2010) Synthesis and grafting of folate–PEG–PAMAM conjugates onto quantum dots for selective targeting of folate-receptor-positive tumor cells. *J Colloid Interf Sci* 350(1):44–50
 8. Das GK, Chan PPY, Teo A, Loo JSC, Anderson JM, Tan TTY (2010) In vitro cytotoxicity evaluation of biomedical nanoparticles and their extracts. *J Biomed Mater Res A* 93A(1):337–346
 9. Chang E, Thekkek N, Yu WW, Colvin VL, Drezek R (2006) Evaluation of quantum dot cytotoxicity based on intracellular uptake. *Small* 2(12):1412–1417
 10. Hsieh SR, Chang CJ, Way TD, Kwan PC, Hung TW (2009) Preparation and non-invasive in-vivo imaging of anti-adhesion barriers with fluorescent polymeric marks. *J Fluoresc* 19(4):733–740
 11. Way TD, Hsieh SR, Chang CJ, Hung TW, Chiu CW (2010) Preparation and characterization of branched polymers as postoperative anti-adhesion barriers. *Appl Surf Sci* 256(10):3330–3336
 12. Pei Q, Yang Y (1996) Efficient photoluminescence and electroluminescence from a soluble polyfluorene. *J Am Chem Soc* 118(31):7416–7417
 13. Feng X, Tang Y, Duan X, Liu L, Wang S (2010) Lipid-modified conjugated polymer nanoparticles for cell imaging and transfection. *J Mater Chem* 20:1312–1316
 14. Stearns V, Schneider B, Henry NL, Hayes DF, Flockhart DA (2006) Breast cancer treatment and ovarian failure: risk factors and emerging genetic determinants. *Nat Rev Cancer* 6:886–893
 15. Slamon D, Godolphin W, Jones L, Holt J, Wong S, Keith D, Levin W, Stuart S, Udove J, Ullrich A (1989) Studies of the HER-2/neu proto-oncogene in human breast and ovarian cancer. *Science* 244(4905):707–712
 16. Slamon D, Clark G, Wong SG, Levin W, Ullrich A, McGuire W (1987) Human breast cancer: correlation of relapse and survival with amplification of the HER-2/neu oncogene. *Science* 235(4785):177–182
 17. Yu D, Hung MC (2000) Role of erbB2 in breast cancer chemosensitivity. *Oncogene* 22(7):673–680
 18. Lee JC, Tsai CY, Kao JY, Kao MC, Tsai SC, Chang CS, Huang LJ, Kuo SC, Lin JK, Way TD (2008) Geraniin-mediated apoptosis by cleavage of focal adhesion kinase through up-regulation of Fas ligand expression in human melanoma cells. *Mol Nutr Food Res* 52(6):655–663
 19. Schwartz BJ (2003) Conjugated polymers as molecular materials: how chain conformation and film morphology influence energy transfer and interchain interactions. *Annu Rev Phys Chem* 54:141–172
 20. Chandler D (2005) Interfaces and the driving force of hydrophobic assembly. *Nature* 437:640–647
 21. Wong KF, Skaf MS, Yang CY, Rossky PJ, Bagchi B, Hu D, Yu J, Barbara PF (2001) Structural and electronic characterization of chemical and conformational defects in conjugated polymers. *J Phys Chem B* 105(26):6103–6107
 22. Martini IB, Smith AD, Schwartz BJ (2004) Exciton-exciton annihilation and the production of interchain species in conjugated polymer films: Comparing the ultrafast stimulated emission and photoluminescence dynamics of MEH-PPV. *Phys Rev B: Condens Matter* B69:035204
 23. Hun X, Zhang Z, Tiao L (2008) Anti-Her-2 monoclonal antibody conjugated polymer fluorescent nanoparticles probe for ovarian cancer imaging. *Anal Chim Acta* 625(2):201–206
 24. Park JW, Hong K, Zalipsky S, Li WL, Carter P, Benz CC, Papahadjopoulos D (1997) Sterically stabilized anti-HER2 immunoliposomes: design and targeting to human breast cancer cells in vitro. *Biochemistry* 36(1):66–75
 25. Fulda S, Debatin KM (2006) Extrinsic versus intrinsic apoptosis pathways in anticancer chemotherapy. *Oncogene* 25:4798–4811
 26. Peralta-Leal A, Rodríguez MI, Oliver FJ (2008) Poly(ADP-ribose) polymerase-1 (PARP-1) in carcinogenesis: potential role of PARP inhibitors in cancer treatment. *Clin Transl Oncol* 10(6):318–323